World Academy of Science, Engineering and Technology
International Journal of Mechanical and Industrial Engineering
Vol:19, No:1, 2025

Kinematic Optimization of Energy Extraction Performances for Flapping Airfoil by Using Radial Basis Function Method and Genetic Algorithm

M. Maatar, M. Mekadem, M. Medale, B. Hadjed, B. Imine

***Abstract*—**In this paper, numerical simulations have been carried out to study the performances of a flapping wing used as an energy collector. Metamodeling and genetic algorithms are used to detect the optimal configuration, improving power coefficient and/or efficiency. Radial basis functions and genetic algorithms have been applied to solve this problem. Three optimization factors are controlled, namely dimensionless heave amplitude h_0, pitch amplitude θ_0, and flapping frequency *f*. ANSYS FLUENT software has been used to solve the principal equations at a Reynolds number of 1100, while the heave and pitch motion of a NACA0015 airfoil has been realized using a developed function (UDF). The results reveal an average power coefficient and efficiency of 0.78 and 0.338 with an inexpensive low-fidelity model and a total relative error of 4.1% versus the simulation. The performances of the simulated optimum RBF-NSGA-II have been improved by 1.2% compared with the validated model.

***Keywords*—**Numerical simulation, flapping wing, energy extraction, power coefficient, energy extraction efficiency, RBF, NSGA-II.

NOMENCLATURE

c	Foil chord length
Cop	Instantaneous power coefficient
Coph	Heave motion instantaneous power coefficient
Coph-mean	Time-averaged power coefficient of heaving motion
Copθ	Pitch motion instantaneous power coefficient
Copθ-mean	Time-averaged power coefficient of pitching motion
Copmean	Time-averaged power coefficient
Cp	Pressure coefficient
CM	Moment coefficient
CY	Lift coefficient
dh/dt	Heaving velocity
dθ/dt	Pitching angular velocity
d	Maximum vertical displacement of the trailing edge
dt	Time step
Er	Relative error
EA	Absolut error
θ0	Pitching amplitude
θ(t)	Pitching motion
ϕ	Phase angle between heaving and pitching motions
Er-T	Total relative error
f	Flapping frequency
FY(t)	Instantaneous vertical force
h0	Dimensionless heaving amplitude
h(t)	Heaving motion
Mz(t)	Instantaneous moment
P	Instantaneous total power extracted
Pa	Total power available in flow
RMSE	Root mean squared error
R2	Coefficient of determination
Re	Reynolds number
St	Strouhal number
T	Flapping period (T = 1/ f)
t	Physical time
U∞	Free stream velocity
Veff	Effective upstream velocity
xp	Chordwise position of pitching axis
αeff	Effective angle of attack
η	Energy extraction efficiency
χ	Feathering parameter

I. INTRODUCTION

THE dependence of humanity on energy is continually increasing due to its consumption in all life aspects [1], which has pushed researchers to find a new and alternative energy sources. The use of renewable energies is on the rise due to their many benefits to humans and the environment, such as reducing pollution and discovering new energy sources [2]. Flapping wings turbine are used to extract energy from water and air; they are characterized by low depths (rivers), slow operating speeds, reduced noise, and small wings. Moreover, oscillating wings have gradually become the focus of numerical and experimental investigations in the last decade [3]. Estimating energy extraction performance using simulation is a process that requires powerful computing resources and is computationally expensive. As a result, optimization methods have been used to obtain good performance prediction at a relatively low numerical cost.

McKinney and DeLaurier pioneered the first energy extraction device using flapping wings [4]. They investigated the possibility of extracting energy using flapping wings by employing a wind-powered mechanical mechanism with an oscillating wing that performs a combined up-and-down motion, were the efficiency reached using this mechanism was 17%. The feasibility of using flapping wings in wind and water turbines has been studied using two-dimensional Navier-Stokes numerical calculations [5]. The results show that employing a non-sinusoidal flapping motion increases the energy extraction

M. Maatar* and B. Imine are with Aeronautics and Propulsive Systems Laboratory, Faculty of Mechanical Engineering, Department of Mechanics, University of Sciences and Technology of Oran Mohamed Boudiaf, BP. 1505 Oran El M'Naouer, 31000 Oran, Algeria (*corresponding author, e-mail: mounir.maatar@univ-usto.dz).

M. Mekadem and B. HADJED are with Laboratory of Fluid Mechanics, Military Polytechnic School (EMP), Bordj El Bahri 16046, Algiers, Algeria.

M. Medale is with IUSTI Laboratory, UMR 7343 CNRS Aix-Marseille University, Chateau-Gombert,13453 MARSEILLE, Cedex 13, France.

performance by 30% compared to wings with a sinusoidal flapping motion. A numerical study of the two-dimensional laminar flow of an oscillating airfoil based on the heaving and pitching motions has been accomplished [6]. The power extraction efficiency exceeded 35% with a maximum effective angle of attack of 35°. The effect of the non-sinusoidal motion trajectory on the energy extraction performance, i.e., extracted power and efficiency, was investigated [7]. Using a pitching trapezoidal trajectory accompanied by a sinusoidal heaving motion significantly increased the energy extracted from the fluid and the efficiency to 63% and 50%, respectively. In a numerical study conducted by [8], the asymmetric time effect of flutter motion on the energy harvesting performance of a flapping wing designed as an energy collector has been tested and under certain configuration parameters it enhances the energy extraction efficiency of the oscillating wing up to 17%. The use of evolutionary algorithms has proven to be effective, maximizing the performance of the flap energy extraction process at a low numerical simulation cost [9]. In the multi-fidelity evolutionary algorithm study, this strategy proved to be more efficient in predicting the kinematic parameters of the motion that maximize the energy extraction efficiency and/or the average power factor. The use of deformable wings has been studied numerically and experimentally to better understand the flow phenomenon around the deformable wing, and the maximum efficiency values are found when the position of the centre of deformation and the position of the flap pivot point coincide [10]. The study of [11] concluded that the optimal kinematic combination parameters of an oscillating wing can be detected efficiently with the given aerodynamic performance using optimization tools based on the regression of a multi-resolution Gaussian process and Bayesian optimization. A study based on optimization methods indicated that the aerodynamic properties and physical fields of an oscillating wing device used as an energy collector can be predicted with accuracy and low computational cost by employing deep learning with a real-time model based on two modular convolutional neural networks [12]. Optimization tools based on informed self-adaptive model has been released, discovering the optimal combination of kinematic parameters for a flapping wing that resulted in an improved time-averaged lift coefficient [13]. A study also showed that the optimal kinematic parameters for flapping wing kinematics were obtained efficiently and quickly using multi-resolution Gaussian process regression and Bayesian optimization [14].

In this work, the energy extraction performances of flapping foil have been studied by using two dimensional numerical simulations. The objectives consist in adopting optimization methodology to find and enhance mean power coefficient and/ or the efficiency of a NACA 0015 flapping wing functioning in extraction regime at a low Reynolds number by using the software ANSYS FLUENT. However, radial basis function coupling with genetic algorithms (NSGA-II) has been applied to identify the optimal configuration of kinematic parameters maximizing the mean power coefficient and/or the efficiency.

II. Flapping Wing Kinematic

A flapping wing executes both heaving and pitching motions. The heaving motion is the vertical wing displacement while the pitching is the wing rotation around a pivot point fixed at x_p distance from the leading edge, as demonstrated in Fig. 1 [6]. However, the flapping motion has been prescribed according to a sinusoidal trajectory. The heaving motion is set corresponding to the following formula given by:

$$h(t) = ch_0 \sin(2\pi ft) \tag{1}$$

The pitching motion is released around a pivot point fixed at one third of the chord from the airfoil leading edge. The foil chord is set to 100 mm. The pitching motion is given by:

$$\theta(t) = \theta_0 \sin(2\pi ft + \phi) \tag{2}$$

The parameters, h_0, θ_0, φ and f are: the dimensionless heaving amplitude; the pitching amplitude; the phase angle between the pitching and heaving motions, and the flapping frequency, consecutively.

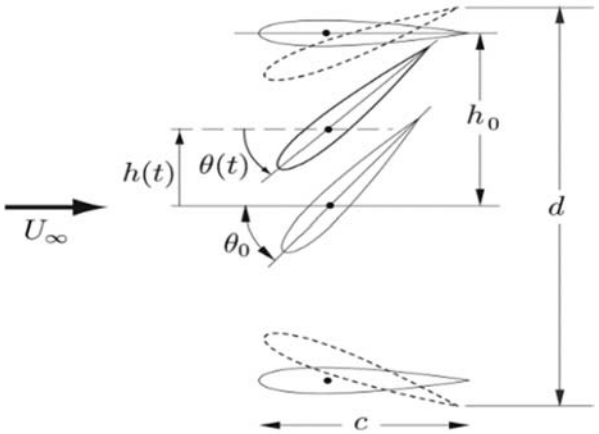

Fig. 1 Flapping wing motion [6]

The Strouhal is a dimensionless number that considers the temporal spatial effect characterizing the energy extraction performances. According to [15], the Strouhal number is given by:

$$St = fd/U_\infty \tag{3}$$

where d represents the maximum excursion of the trailing edge defined as follows:

$$d = ch_0 + 2(c - x_p)\sin\theta(t) \tag{4}$$

However, x_p represents the chordwise position of pitching axis.

The induced, effective angle of attack α_{eff} and the effective upstream velocity V_{eff} due to vertical displacement of the wing in the flow are expressed according to [6] as follows:

$$\alpha_{eff} = \arctan(-\frac{dh/dt}{U_\infty}) - \theta(t) \quad (5)$$

$$V_{eff} = \sqrt{U_\infty^2 + (dh(t)/dt)^2} \quad (6)$$

The maximum values of α_{eff} and V_{eff} in a flapping period have an important effect on the aerodynamic performances and the behaviour of the flow around the wing.

The functioning regime of flapping wings has been fixed according to the feathering parameter value [15]. The feathering parameter χ is expressed as follows:

$$\chi = \frac{\theta_0}{\arctan(ch_0 w / U_\infty)} \quad (7)$$

The resulting aerodynamic force is in the same direction as the vertical displacement of the wing when operating in extraction regimes [6].

III. Performance of Energy Extraction

The instantaneous power extracted in a flapping period from the heave and pitch motion is expressed through the instantaneous power coefficient which is equal to:

$$Cop = \frac{P}{0.5\rho U_\infty^3 c} \quad (8)$$

Otherwise, it is defined as:

$$Cop = \frac{C_Y(t)}{U_\infty}\frac{dh(t)}{dt} + \frac{C_M(t)}{U_\infty}\frac{d\theta(t)}{dt} = Cop_h + Cop_\theta \quad (9)$$

where the lift and the moment coefficients are expressed respectively by:

$$C_Y(t) = \frac{F_Y(t)}{1/2\rho U_\infty^2 S} \quad (10)$$

$$C_M(t) = \frac{M_z(t)}{1/2\rho U_\infty^2 S} \quad (11)$$

The average mean power during one cycle is defined as:

$$\overline{P} = \frac{1}{T}\int_0^T P dt \quad (12)$$

while the mean power coefficient is given by:

$$Cop_{mean} = \frac{\overline{P}}{0.5\rho U_\infty^3 c} \quad (13)$$

The energy extraction efficiency is expressed with:

$$\eta = \frac{\overline{P}}{P_a} = Cop_{mean}\frac{c}{d} \quad (14)$$

where, the total power in flow P_a is given by:

$$P_a = \frac{1}{2}\rho U_\infty^3 d \quad (15)$$

IV. Optimization Methods

According to [16], a mathematical formulation of an optimization problem is given as:

$$\begin{cases} Min(Y_1(x), Y_2(x)..., Y_n(x)) \\ x = (x_1, x_2, x_3, ..., x_k) \\ x_{\min} < x < x_{\max} \end{cases} \quad (16)$$

The adopted optimization approach uses a radial basis function coupled with genetic algorithm. The aim of the first method is to find a metamodel *Y(x)* basing on RBF method, where the second one reposes on the application of GAs in order to maximize the found objective function.

Approximation of the Objective Function by RSM

The principle of RSM is to replace the real function Y(x), which is evaluated by experiments, with an approximate function $\hat{Y}(x)$ according to a design experiment [17].

Radial Basis Function Approximation

The aim of the RBF method is to find an approximation of the search function through a set of master points using the Euclidean distance [18].

Maximization of Objective Function Using Genetic Algorithm

The approximate objective function $\hat{Y}(x)$ has been adopted to find the optimum using GAs in the chosen search intervals. GAs were first developed and popularized by [19] and [20].

V. Results and Discussion

Numerical Approach Validation

The validation of the adopted numerical approach has been performed against the work of [6] in the early works [21]. The numerical simulations are conducted for a NACA 0015 airfoil at a Reynolds number of 1100, with a reduced frequency f^* of 0.14, pitching amplitude of 76.33°, plunging amplitude $h_0 = 1$, position of pivot point $x_p = 0.33$c, phase angle ϕ of 90°, and a time step of $0.0005T$.

Consistency of the RBF-NSGAII Optimization Technique

In order to validate the proposed optimization method, the algorithm was tested using a known mathematical function. In the first step, we searched for the Pareto front using the NSGA-

II method alone without using the metamodel, which requires the use of the exact (mathematical) function for the evaluation of the objective functions. In the second step, we used the NSGA-II method coupled with RBF method, i.e., using the metamodel to evaluate the objective functions. The validation of the optimization method was performed as follows:

Test Problem

FON is a two objective optimization problem cited by [22]. In this test, the mathematical function is bi-objective with six optimization variables.

$$\begin{cases} f_1(\mathrm{x}) = 1 - \exp\left(-\sum_{i=1}^{6}\left(x_i - 1/\sqrt{6}\right)^2\right) \\ f_2(\mathrm{x}) = 1 - \exp\left(-\sum_{i=1}^{6}\left(x_i + 1/\sqrt{6}\right)^2\right) \\ x_i \in [-1,1] \quad \forall\, i = 1,\ldots,6 \end{cases}$$

The initial size of the master points is N = 30. The results obtained after 68 exact evaluations are shown in Fig. 2.

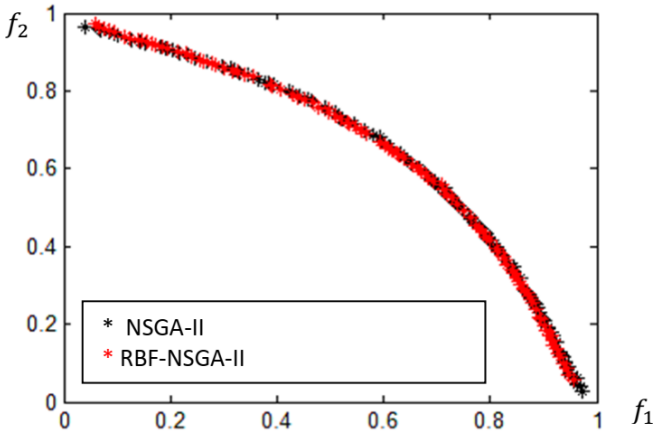

Fig. 2 Pareto front of the test problem

The results of the adopted function test confirm the perfect prediction of the RBF metamodel of the solution (Pareto front) of the test optimization problems, the front obtained by using the RBF metamodel is very close to that obtained by using the exact function only, so it is possible to replace the exact evaluations of the objective function by approximate solutions using the RBF metamodel.

Performances Maximization Using RBF-NSGAII Model

The aim of this part of the study is to find the optimal configuration of kinematic motion parameters maximizing the energy extraction performance of a NACA 0015 flapping wing with a chord length of 0.1 c. The optimization variables are the dimensionless heave amplitude h_0, the pitch amplitude θ_0, and the flapping frequency f. It should be noted that the simulation time step is $0.01T$ in accordance with the study by Mekadem et al. [23] to ensure rapid prediction of the performances. The search intervals for the optimization factors are the same used for the Box-Behnken-NSGA-II optimization method [21]. According to (16), the optimization problem in this part of the study is given as:

$$\begin{cases} Min(Cop_{moyen}(x), \eta(x)) \\ x = (h_0, \theta_0, f) \\ 0.7 \le h_0 \le 1.3 \\ 1.33(76°) \le \theta_0 \le 1.5(86°) \\ 0.25 \le f \le 0.35 \end{cases} \quad (17)$$

Objective Function Approximation Using RBF

The RBF method approximates the objective function by learning from networks in hidden layers, using simulated master points and refinement points.

Validation of the RBF-NSGAII Methodology

Another validation of the RBF-NSGAII method is carried out by calculating the total relative error between the RBF-NSGAII model and the numerical simulation as a function of the number of refinements (Fig. 3). The results presented in the figure show that after the first refinement of the solution, the total relative error obtained between the RBF-NSGAII model and the simulation is less than 0.15%. The good convergence and stabilization of the calculated errors towards minimum values of 0.0038% as the number of refinements increases, confirms the credibility of the adopted method RBF-NSGAII (Fig. 3). The flexibility of the method in the transition between the fundamental operators (exploration and exploitation) characterized by the jump between the peaks of the maximum and minimum errors of several refinement steps, confirms the robustness of the method in balancing between exploration and exploitation in search of the global optimum, and avoiding local optima while respecting the stopping criterion imposed by the fixed total relative error.

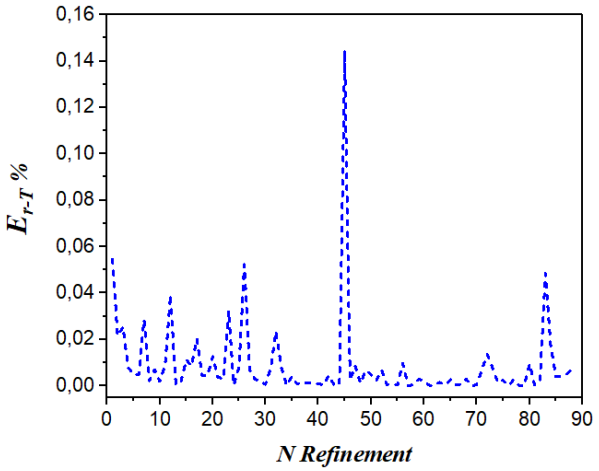

Fig. 3 Relative error of, efficiency, Cop_{mean} and Total relative error as a function of number refinement

Fig. 4 (a) shows the points predicted by the RBF-NSGAII model and those obtained by simulation. The superposition of several points of the two models compared is appropriate to the minimal relative errors between the two methods. This is attributed to the exploitation of neighboring regions around the local optima predicted by the RBF-NSGAII method and those

of the simulation. Conversely, the distance between the points of the two models is characterized by considerable errors, resulting from the exploration operations in distant regions of the local optima predicted by the RBF-NSGAII method and those of the simulation.

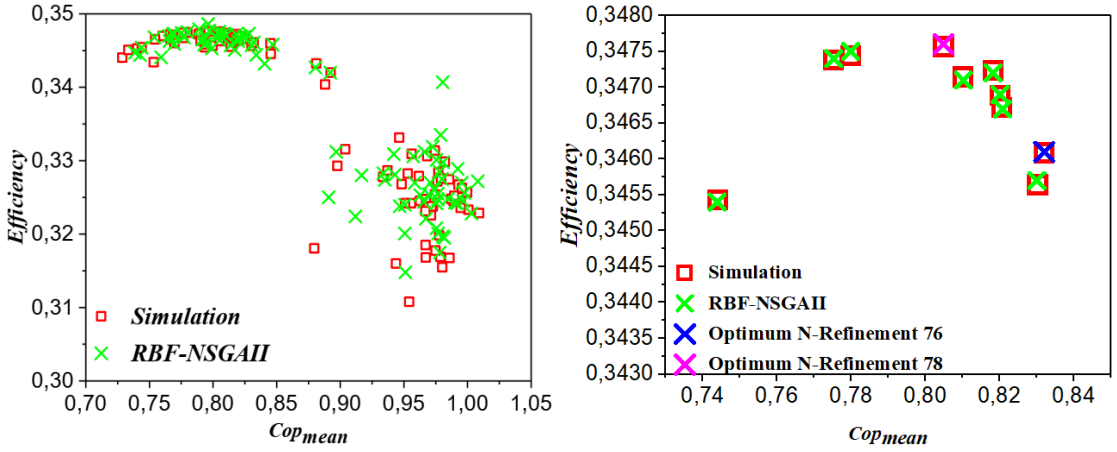

(a) (b)

Fig. 4 Performance obtained from simulation versus RBF-NSGAII: (a) All configurations, (b) Zoom on the optimum zones

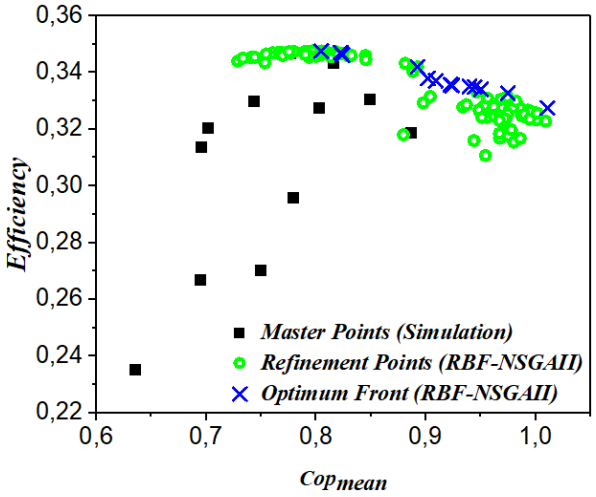

Fig. 5 Performance of master points (simulation), refinement points (simulation) and the Pareto front predicted by RBF-NSGAII

Fig. 4 (b) shows the 10 best solutions chosen with a total error less than 0.027%. The performances detected by the RBF-NSGAII model are very close to those of the simulation and all points are capped by the predicted optimum using the RBF-NSGAII model and that of the simulation obtained in refinement step number 78.

The optimum of this step number has been selected to be analyzed in the next section due to its higher efficiency, as shown among the best solutions summarized in Table I.

Fig. 5 shows the performance (average power coefficient and efficiency) of the master points (12 points), the refinement points (88 points), and the Pareto front at refinement step number 78. It can be seen that the 12 master points, randomly selected according to the Latin Hyper Cube (LHD) experimental design, are scattered throughout the search space, while the refinement points are concentrated above the optimal Pareto front detected by the RBF-NSAII method.

In Table I, the 10 best solutions (optimums) detected by the RBF-NSGAII method and those obtained from the simulation classified according to the criterion of minimum total relative error between optimization (RBF-NSGAII) and simulation which does not exceed 0.0038%. This error rate has been selected to give sufficient time to the process of refining the solution (maximizing the objective functions) and improving precision, ensuring that the RBF-NSGAII model becomes reliable.

TABLE I
TEN BEST CONFIGURATIONS PREDICTED BY SIMULATION AND RBF-NSGAII METHOD WITH THREE OPTIMIZATION VARIABLES AT TIME STEP OF $0.01T$

	N Refinement	h_0	f	θ_0	Cop_{mean} Simulation	η Simulation	Cop_{mean} RBF-NSGAII	η RBF-NSGAII	E_{r-T} %
1	**76**	**0.87988**	**0.33654**	**80**	**0.83201**	**0.34609**	**0.832**	**0.3461**	**0.0038**
2	79	0.85522	0.33505	80	0.82009	0.34689	0.8201	0.3469	0.00418
3	69	0.77863	0.32725	79	0.77527	0.34738	0.7753	0.3474	0.00593
4	57	0.85054	0.33166	80	0.8183	0.34724	0.8183	0.3472	0.01095
5	**78**	**0.83125**	**0.3269**	**79**	**0.80494**	**0.34756**	**0.8049**	**0.3476**	**0.01143**
6	34	0.78696	0.32573	79	0.77986	0.34744	0.7799	0.3475	0.01754
7	43	0.84227	0.33269	79	0.81017	0.34715	0.8103	0.3471	0.02118
8	61	0.87864	0.31863	80	0.83025	0.34564	0.8301	0.3457	0.02448
9	55	0.72822	0.32998	79	0.74408	0.34543	0.7439	0.3454	0.02576
10	81	0.85733	0.32057	80	0.82005	0.34637	0.8199	0.3463	0.02617

Checking Optimal Configuration with Simulation

The detected optimal configuration using RBF-NSGA-II (Cop_{mean} = 0.8049 and η = 0.3476) have been checked by the simulation adopting a time step of 0.0005T (Table II). The results show, an average power coefficient and efficiency of 0.78 and 0.338. The found results show that the RBF-NSGA-II detect the optimal performances at low computational cost and with a total relative error of 4.1% compared to the simulation which confirms the reliability of the adopted optimization methodology.

TABLE II
CHECKING OPTIMAL PERFORMANCES BY SIMULATION

	Cop_{mean}	η	E_{r-T}
Simulated Optimum RBF-NSGA-II(dt = 0.0005T)	0.78	0.338	
RBF-NSGA-II(dt = 0.01T)	0.8049	0.3476	
Simulated Optimum VS RBF-NSGA-II	3.1%	2.8%	4.1%

Force Coefficient Comparison

A comparison of the results between the simulated optimum RBF-NSGAII (Case 2) and the validated model (Case 1) has been performed. Simulations were conducted with a time step of 0.0005T. The results for the coefficients of the forces Cx, Cy and Cm of the two compared cases are shown in Figs. 6-8. It is evident that the drag coefficient of the simulated optimum obtained in case 2 is higher than that of the validated model (see Fig. 6). This deference is attributed to the pitch amplitude value of 80° detected in case 2, which is higher than the 73.22° used in the validated model.

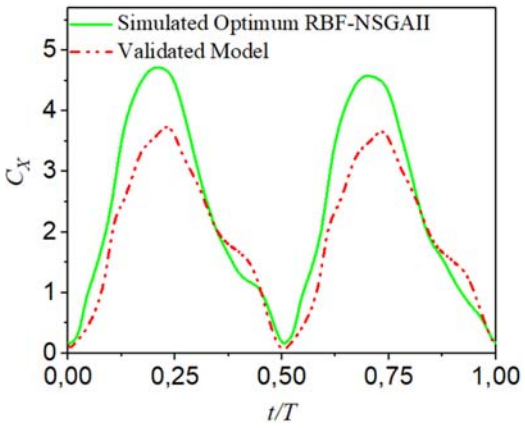

Fig. 6 Drag coefficient over one flapping period of the simulated optimum RBF-NSGAII, and the validated model

For the lift coefficient (Fig. 7), the simulated optimum (RBF-NSGAII) shows a slightly higher value compared to the validated model at and around times 0.125T (0.125T+0.5T). However, this slight difference become negative around time 0.4T (0.4T+0.5T) when compared to the validated model.

With regard to the moment coefficient (Fig. 8), the results show that the moment coefficient of RBF-NSGAII model exceeds that of case 1 (the validated model) in most of the interval, particularly at 0.0625T (0.0625T+0.5T) and surrounding times.

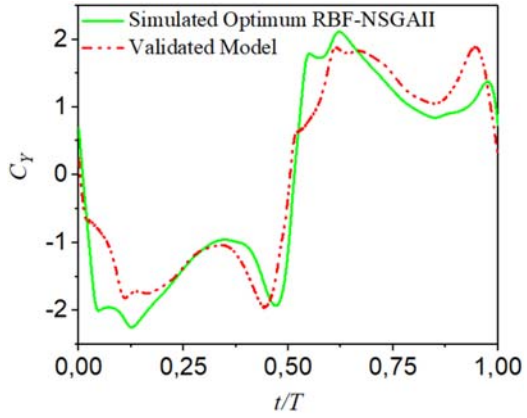

Fig. 7 Lift coefficients over a flapping period for the simulated optimum RBF-NSGAII, Box-Behnken, and the validated model

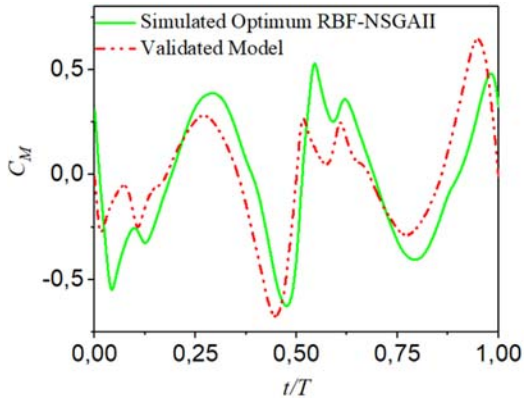

Fig. 8 Momentum coefficient over a flapping period of the simulated optimum RBF-NSGAII and validated model

The effective angle of attack α_{eff} for the simulated optimum RBF-NSGAII (38.07°) is higher than that of the validated model (34.99°), however the effective velocity V_{eff} is slightly lower for case 2 than for case 1 (Fig. 9). In fact, the average power coefficient has decreased by 5.68% (Table III), whereas the energy extraction efficiency has improved by 1.2%. This improvement is justified by the greater angle of attack for the second case, which plays a dominant role in this improvement.

Energy Performances Comparison

The coefficients Cop_h Cop_θ and Cop represent the power coefficients due to the motion of heave pitch and flap, respectively, for the simulated optimum of the RBF-NSGAII and the validated model (Figs. 10-12).

TABLE III
ENERGY EXTRACTION PERFORMANCES OF THE COMPARED CASES

	Cop_{h-mean}	$Cop_{\theta-mean}$	Cop_{mean}	η	E_{r-T}	d
Case 1 (dt = 0.0005T)	0.795	0.062	0.856	0.334		0.256
Case 2 (dt = 0.0005T)	0.82	-0.04	0.78	0.338		0.231
Contribution Cop_{h-mean}, $Cop_{\theta-mean}$	105.13%	-5.13%	100%			
Enhancement Case 2 vs. Case 1	3.14%	-400%	-5.68%	1.2%	5.8%	

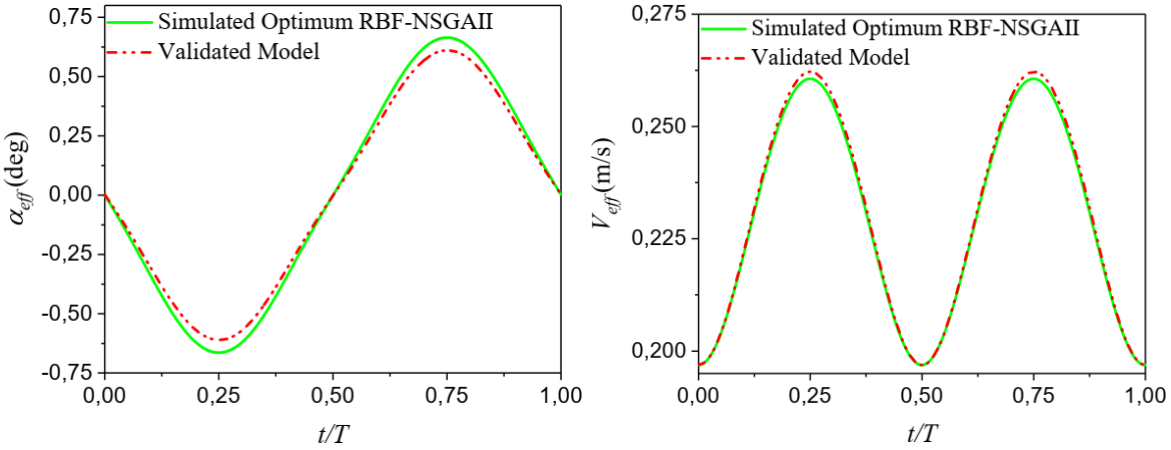

(a) (b)

Fig. 9 (a) Effective angle of attack and (b) Effective velocity over a flapping period of the, simulated optimum RBF-NSGAII and validated model

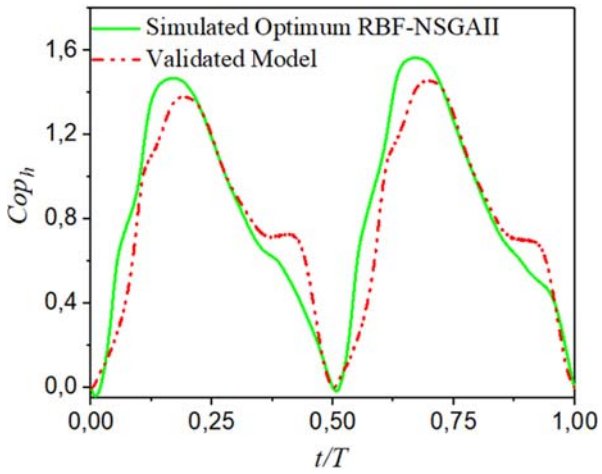

Fig. 10 Instantaneous power coefficients Cop_h of the simulated optimum RBF-NSGAII and validated model

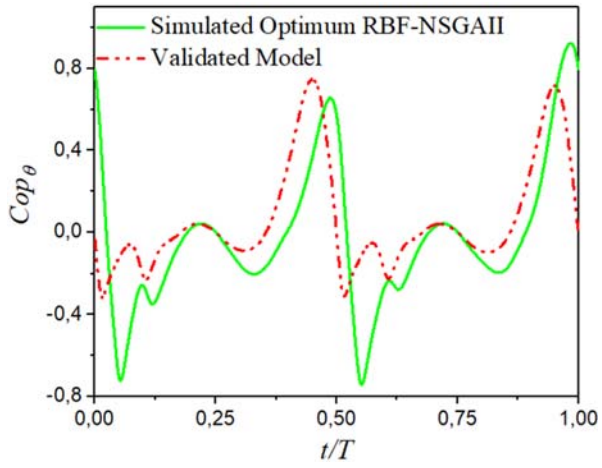

Fig. 11 Instantaneous power coefficients Cop_θ of the simulated optimum RBF-NSGAII and validated model

In the light of the results in Fig. 10, the Cop_h of case 2 exceeds that of case 1 in most of the period, except at 0.0625 (0.0625+0.5T), 0.1875T (0.1875T +0.5T), 0.375 (0.375+0.5T). This observation is further highlighted by the total average power coefficient Cop_{mean} presented in Table III, which shows a value of 0.82 for case 2 versus 0.795 for case 1, reflecting an improvement of Cop_{mean} of 3.14% compared case 2 to case 1. Additionally, the Cop_h has positively contributed 105.13% to the total power coefficient Cop_{mean} over the flapping period.

Regarding the Cop_θ of case 2 (Fig. 11), it shows improvement around the instants 0.0625 (0.0625+0.5T) and 0(T) compared to case 1. However, a degradation of the Cop_θ for case 2 is observed around 0.45T. Overall, the $Cop_{\theta-mean}$ of case 2 experienced a 400% reduction compared to $Cop_{\theta-mean}$ for case 1 (see Table III), indicating a negative contribution of 5.13% to the total power coefficient.

Fig. 12 highlights the improvement in efficiency despite the degradation in the power coefficient when comparing case 2 to case 1. This improvement is captured by (14), which shows efficiency of energy extraction is inversely proportional to the factor "d" (maximum trailing edge excursion), as detailed in Table III.

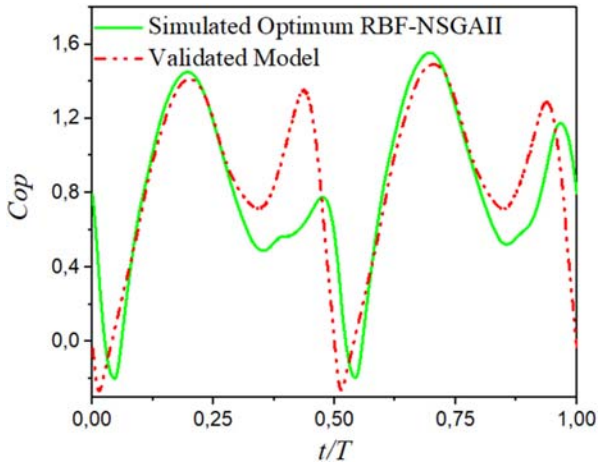

Fig. 12 Instantaneous power coefficients Cop of the simulated optimum RBF-NSGAII and validated model

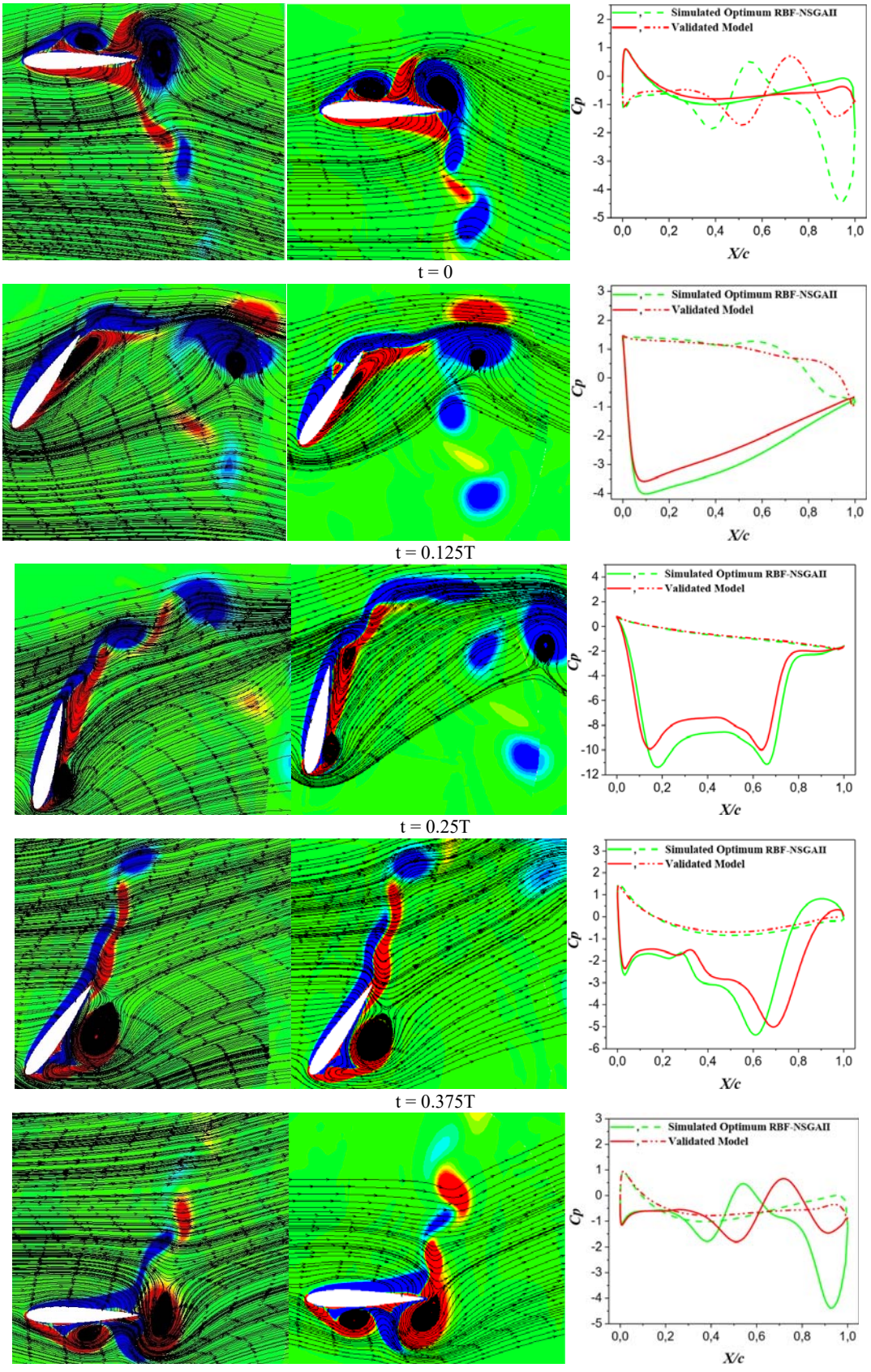

Fig. 13 Instantaneous vortex contour, (a) Validated model, (b) Simulated RBF-NSGAII optimum, (c) pressure coefficients, for both compared cases at selected times over half period: the solid and dotted lines show the pressure on the lower and upper surface

Vorticity and Pressure Coefficients Comparison

It is also important to note that the vortex contours and pressure coefficients in the other half-period are symmetrical but inverted relative to this half-period. Fig. 13 shows the vortex structures, where we can clearly see that the vortices of the two cases are almost identical, with minor variations in intensity and position for case 2. These differences can be attributed to the increased angle of attack for case 2. Additionally, the pressure coefficients show an increase for nearly the entire half-period for case 2 compared to case 1, which explains the improved efficiency for the second case.

VI. Conclusion

The aim of this numerical study is to predict and maximize the efficiency of NACA 0015 flapping airfoil utilizing metamodeling and genetic algorithms. The 2-D numerical simulations were conducted to calculate the mean coefficient power and/or efficiency. The optimization methodology employed achieved a mean power coefficient and efficiency of 0.78 and 33.8%, with an inexpensive simulation cost and a total relative error of 4.1% compared to the simulation. The average power coefficient and efficiency of the simulated optimum has been improved by 1.2% compared to the validated model. The optimal kinematic parameters are a dimensionless heaving amplitude of 0.831c, pitching amplitude of 80°, and a low flapping frequency of 0.327 Hz. The obtained results reveal that:

1. The majority of the extracted energy is attributed to the heave motion;
2. The dominant factor enhancing energy extraction performance is the effective angle of attack of 38.07°;
3. The metamodel for the three optimization factors was built using 12 simulation points, demonstrating an inexpensive and low-fidelity approach.

Future work will focus on identifying the optimal configuration for a larger number of kinematic parameters, introducing the effect of non-sinusoidal flapping trajectory, and exploring different NACA airfoils, in order to maximize the performance of energy extraction from a flapping wing. In addition, a comparative study between the RBF-NSGAII and Box-Behnken-NSGAII methods will be conducted to evaluation optimization solutions and method performance.

Acknowledgments

The IUSTI laboratory Aix-Marseille University was part of this research, we express our gratitude for Professor Marc MEDALE and JOBIC Yann for their contributions and precious helps in this study, and laboratory staff for the programming learning opportunities.

References

[1] B. Xu, Q. Ma, and D. Huang, "Research on energy harvesting properties of a diffuser-augmented flapping wing," *Renew. Energy*, vol. 180, pp. 271–280, Dec. 2021, doi: 10.1016/j.renene.2021.08.053.

[2] P. Ma, Y. Wang, Y. Xie, and J. Zhang, "Analysis of a hydraulic coupling system for dual oscillating foils with a parallel configuration," *Energy*, vol. 143, pp. 273–283, Jan. 2018, doi: 10.1016/j.energy.2017.10.141.

[3] B. Zhu, Y. Huang, and Y. Zhang, "Energy harvesting properties of a flapping wing with an adaptive Gurney flap," *Energy*, vol. 152, pp. 119–128, Jun. 2018, doi: 10.1016/j.energy.2018.03.142.

[4] W. McKinney and J. DeLaurier, "Wingmill: An Oscillating-Wing Windmill.," *AIAA Pap.*, vol. 5, no. 2, pp. 80–87, 1980.

[5] M. F. Platzer, M. a Ashraf, J. Young, and S. Lecturer, "Wind and Hydropower Generator," *New Horizons*, no. January, pp. 1–13, 2009.

[6] T. Kinsey and G. Dumas, "Parametric study of an oscillating airfoil in a power-extraction regime," *AIAA J.*, vol. 46, no. 6, pp. 1318–1330, 2008, doi: 10.2514/1.26253.

[7] Q. Xiao, W. Liao, S. Yang, and Y. Peng, "How motion trajectory affects energy extraction performance of a biomimic energy generator with an oscillating foil?," *Renew. Energy*, vol. 37, no. 1, pp. 61–75, 2012, doi: 10.1016/j.renene.2011.05.029.

[8] J. Zhu and T. Tian, "The time asymmetric pitching effects on the energy extraction performance of a semi-active flapping wing power generator," *Eur. J. Mech. B/Fluids*, vol. 66, pp. 92–101, 2017, doi: 10.1016/j.euromechflu.2017.06.006.

[9] Z. Liu, K. S. Bhattacharjee, F. Tian, J. Young, T. Ray, and J. C. S. Lai, "Kinematic optimization of a flapping foil power generator using a multi-fidelity evolutionary algorithm," 2018, doi: 10.1016/j.renene.2018.08.015.

[10] B. Zhu, "Energy extraction properties of a flapping wing with an arc-deformable airfoil Energy extraction properties of a flapping wing with an arc-deformable airfoil," vol. 023302, no. November 2018, 2019, doi: 10.1063/1.5079864.

[11] H. Zheng, F. Xie, T. Ji, Z. Zhu, and Y. Zheng, "Multifidelity kinematic parameter optimization of a flapping airfoil," *Phys. Rev. E*, vol. 101, no. 1, Jan. 2020, doi: 10.1103/PhysRevE.101.013107.

[12] Y. Li, T. Liu, Y. Wang, and Y. Xie, "Deep learning based real-time energy extraction system modeling for flapping foil," *Energy*, vol. 246, no. 123390, 2022, doi: 10.1016/j.energy.2022.123390.

[13] T. J. and Y. Z. Zheng H., F. Xie, "Kinematic parameter optimization of a flapping ellipsoid wing based on the data-informed self-adaptive quasi-steady model," *Phys. Fluids*, vol. 32, no. 4, p. 041904, Apr. 2020, doi: 10.1063/1.5144642.

[14] T. (季廷炜) Ji, F. (金凡) Jin, F. (谢芳芳) Xie, H. (郑鸿宇) Zheng, X. (张鑫帅) Zhang, and Y. (郑耀) Zheng, "Active learning of tandem flapping wings at optimizing propulsion performance," *Phys. Fluids*, vol. 34, no. 4, p. 47117, Apr. 2022, doi: 10.1063/5.0084160.

[15] J. M. Anderson, K. Streitlien, D. S. Barrett, and M. S. Triantafyllou, "Oscillating foils of high propulsive efficiency," *J. Fluid Mech.*, vol. 360, pp. 41–72, 1998, doi: 10.1017/S0022112097008392.

[16] R. T. Haftka, "Response surface approximations for structural optimization W. J. Roux AIAA, NASA, and ISSMO, Symposium on Multidisciplinary Analysis and Optimization, Response Surface Approximations for," pp. 565–578, 1996.

[17] R. H. Myers, D. C. Montgomery, G. Geoffrey Vining, C. M. Borror, and S. M. Kowalski, "Response Surface Methodology: A Retrospective and Literature Survey," *J. Qual. Technol.*, vol. 36, no. 1, pp. 53–78, 2004, doi: 10.1080/00224065.2004.11980252.

[18] A. G. Bors, "Introduction of the Radial Basis Function (RBF) Networks," *Online Symp. Electron. Eng.*, vol. 1, no. 1, pp. 1–7, 2001.

[19] J. H. Holland, "even their creators do not fully understand Genetic Algorithms n," *Sci. Am.*, vol. 267, no. 1, pp. 66–73, 1992.

[20] Goldberg D. E., "The Design of Innovation. Technol," *Technol. Forecast. Soc. Chang.*, vol. 64, no. 7, p. 12, 2000.

[21] M. Maatar, M. Mekadem, M. Medale, and B. Imine, "Kinematic Optimization of Energy Extraction Efficiency for Flapping Airfoil by using Response Surface Method and Genetic Algorithm," *J. Appl. Fluid Mech.*, vol. 16, no. 5, pp. 932–946, 2023, doi: 10.47176/jafm.16.05.1652.

[22] K. Deb, A. Pratap, S. Agarwal, and T. Meyarivan, "A fast and elitist multiobjective genetic algorithm: NSGA-II," *IEEE Trans. Evol. Comput.*, vol. 6, no. 2, pp. 182–197, 2002, doi: 10.1109/4235.996017.

[23] M. Mekadem, T. Chettibi, S. Hanchi, L. Keirsbulck, and L. Labraga, "Kinematic optimization of 2D plunging airfoil motion using the response surface methodology," *J. Zhejiang Univ. Sci. A*, vol. 13, no. 2, pp. 105–120, 2012, doi: 10.1631/jzus.A1000502.